

Mechanisms of megaripple generation: from dunes to megaripples

D. Idier⁽¹⁾ and D. Astruc⁽²⁾

(1) University of Twente, Group Water Engineering and Management. PO Box 217 – 7500 AE Enschede, the Netherlands. d.idier@ctw.utwente.nl.

(2) IMFT, allée Pr. Camille Soula, 31400 Toulouse, France. astruc@imft.fr.

Abstract

Richards (1980) conjectured that megaripples are generated by the same instability processes as ripples but in the presence of small seabed ripples. Towards a better understanding of megaripples formation process, a morphodynamical numerical model is used to investigate the bed roughness influence on the steady current-induced linear stability of a sandy bed. For a ripple-free bottom and a water depth of 30 m, the model leads to the formation of dunes of 400 m wavelength whereas megaripples of 20 m wavelength are generated for a bed roughness height of about 1 m. These results could explain the presence of megaripples on flat bed, in very shallow-waters, but also the presence of megaripples on larger dunes.

1. Introduction

In the south of the North Sea by dunes having wavelength of several hundred meters and being often covered by smaller bedforms called megaripples (Fig. 1). As a generic name, these two kinds of bedforms can be called sandwaves. To distinguish them, some classification is required and here the terms dunes, megaripples or ripples, will be used, depending on their spatial scale (Tab. 1). The dunes have heights up to several meters and their migration rate may reach 100 m/y (Stride, 1982). They are commonly covered by megaripples whose migration rate can reach 1 m/h (Idier et al., 2002). However, megaripples can also be observed on flat seabed, mainly in shallow water. Both of these bedforms are most of time covered by even smaller bedforms, called ripples.

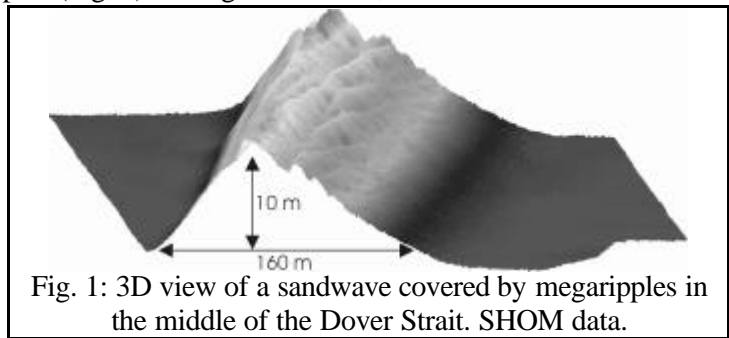


Fig. 1: 3D view of a sandwave covered by megaripples in the middle of the Dover Strait. SHOM data.

The prediction of the temporal evolutions of the height and position of the largest structures is of practical importance for various applications, including navigation safety.

	Ripples	Megaripples	Dunes
Height (m)	<0.06	0.06-2	2-15
Wavelength (m)	<0.6	0.6-20	20-1000
Roughness height k_s (m)	0.2 to 0.3 (vortex)	0.3 to 4	4 to 15

Tab. 1 – Bedform classification and bed roughness height, from (Dalrymple et al., 1978 ; Van Rijn, 1989).

A first approach has been to relate the bed shear stress to the bedforms. This has been done mainly by flume experiments. From van Rijn (1993), for particle diameter parameter smaller than 10 and a Froude number smaller than 0.8, the bedforms should be classified as follow, depending on the value of the bed shear stress parameter $T (= (\tau_b - \tau_c) / \tau_c)$: $0 < T < 3$ (mini-ripples), $3 < T < 10$ (megaripples and dunes), $10 < T < 15$ (dunes), $15 < T$ (sandwaves). However, it is worthwhile to notice that in this approach, the bed

shear stress parameter is estimated for already existing fully developed bedforms. Thus, this provides no information on the bed shear stress required for ripples, megaripples or dune generation.

As a first step in the analysis of the generation these bedforms, some insights have been gained by linear stability analysis. Richards (1980) and Hulscher (1996) showed that both dunes and ripples may result from free instabilities developing on the interface between the seabed and the 3-dimensional current. For symmetrical tidal currents, the bedform generation results from an unbalance between tidal averaged flow-driven sediment fluxes converging toward the crest (bedform growth) and gravity-driven sediment fluxes diverging from the crest (bedform damping) (Hulscher, 1996). Using the Navier-Stokes equations and a constant viscosity to model turbulent motions, Hulscher (1996) showed that the linearly most amplified mode has a wavelength similar to the observed dunes wavelength. Richards (1980) performed a similar analysis for a steady current, using a vertically non-uniform turbulent viscosity model, and obtained two unstable modes: one corresponding to ripples and the other to dunes. For increasing bed roughness, the ripple mode wavelength increases whereas the dune mode wavelength decreases. For large enough bed roughness, the ripple and dune modes coalesce in a single mode. As a remark, Richards (1980) conjectured that megaripples might result from the ripple mode, with a wavelength increase in the presence of smaller ripples on the seabed. However, none of these authors discuss in detail the megaripple generation mechanisms.

In this study, using numerical modeling, we focus on the linear regime of the bottom instability to analyze the possible influence of bed roughness on possible megaripple generation. The stability properties of a flat bed subject to a steady current are investigated for a bed roughness varying from grain roughness to form roughness height of about 1 m.

2. Morphodynamical model and computation parameters

This study is based on numerical modeling, an approach which already proved to give good results in the study of sandbank generation (Idier and Astruc, 2003a).

2.1 Model

The hydrodynamical model relies on the 3D Navier-Stokes equations. The vertical turbulent viscosity is parameterized by a mixing length model. A classical bottom friction parametrization is used:

$$\bar{\tau}_b = \mathbf{r} \frac{\|\bar{\mathbf{u}}\|^2}{C^2} \frac{\bar{\mathbf{u}}}{\|\bar{\mathbf{u}}\|} \quad \text{with} \quad C = (1/\mathbf{k}) \ln \Delta Z / z_0 \quad (1)$$

where \mathbf{r} is the water density, $\bar{\mathbf{u}}$ the near-bed velocity and C the friction coefficient. C depends on the Karman constant ($\mathbf{k} = 0.41$), the bed roughness length z_0 and a characteristic length ΔZ (one tenth of the height of the first grid cell above the bottom (Janin et al., 1997)). The bed roughness length z_0 is related to the bed roughness height k_s by $z_0 = k_s / 30$. This bed roughness height is the sum of a grain roughness height k_{bs} and of a form roughness height k_{bf} such that:

$$k_b = k_{bs} + k_{bf} \quad \text{with} \quad k_{bs} = 3D_G \quad \text{for} \quad D_G = 0.3 \text{ mm} \quad \text{and} \quad k_{bf} = 20\mathbf{g}H_r(H_r/I_r) \quad (2)$$

D_G is the grain size, H_r and I_r are the height and the wavelength of the small scale bedforms and \mathbf{g} is a coefficient equal to 1 for a bed with ripples only (van Rijn, 1993).

The bottom evolution model is based on the sediment mass conservation, which relates the bed temporal evolution to the spatial variations of the sediment flux:

$$\frac{\partial h}{\partial t} + \frac{1}{1 - \mathbf{e}_p} \bar{\nabla} \cdot \bar{\mathbf{S}}_b = 0 \quad (3)$$

with h the bed level, \mathbf{e}_p the bed porosity and $\bar{\mathbf{S}}_b$ the sediment flux. Both bed load and gravity driven sediment fluxes are taken into account:

$$\bar{S}_b = \mathbf{a} (\|\bar{\mathbf{t}}_b\| - \mathbf{t}_c)^b (\bar{\mathbf{t}}_b / \|\bar{\mathbf{t}}_b\| - \mathbf{b} \bar{\nabla} h) (\|\bar{\mathbf{t}}_b\| - \mathbf{t}_c) \quad (4)$$

\mathbf{t}_c is the critical bed shear stress, H is an Heaviside function and \mathbf{b} is the bed slope coefficient, equal to the co-tangent of the stability angle of the sediment. b and \mathbf{a} are computed from the Van Rijn formula (1993):

$$b = 2.1 \text{ and } \mathbf{a} = 0.053 \sqrt{(s-1)g} D_G^{1.5} D_*^{-0.3} \mathbf{t}_c^{-2.1} \quad (5)$$

with $s = \mathbf{r}_s / \mathbf{r}$ the relative density, $D_* = D_G ((s-1)g/\mathbf{n}^2)^{1/3}$ the particle parameter and \mathbf{n} the water molecular viscosity.

In this model, the grain size influences both the bed shear stress (1) and the sediment flux (5), whereas small-scale bedforms geometry influences only the bed shear stress (1). To compute the flow, the sediment flux and the bed evolution, the *Telemac* finite element software is used, as for previous sandbanks dynamics studies (Idier and Astruc, 2003a).

2.2 Bed perturbation

As the spatial scales under consideration are small, the Coriolis force is neglected and the dune crests are likely to be perpendicular to the current (Hulscher, 1996). Thus, we study the time evolution of small amplitude sinusoidal bedforms $h_1(x,t)$ perpendicular to the current, superimposed to a flat bed, which is subject to a main steady flow \mathbf{t}_{b0} (depth-averaged velocity $U = 1 \text{ m/s}$, in the x -direction). This bed perturbation induces a first order bed shear stress perturbation \mathbf{t}_{b1} to the mean bed shear stress \mathbf{t}_{b0} , $\mathbf{t}_{b1} = |\mathbf{t}_{b1}| \cos(kx + \mathbf{j})$ with $k = 2\mathbf{p}/\mathbf{l}$ the bed perturbation wave number and \mathbf{j} the spatial phase-lag between the bed shear stress and the bed perturbation, such that a positive phase-lag implies a bed shear stress perturbation maximum located upstream of the bedform crest. As shown by Hulscher (1996), among all the modes, there is one, which is the linearly most amplified mode (LMA mode).

2.3 Parameters and related bedforms regimes

The physical parameter values are those of dunes areas located in the Dover Strait: water depth $H = 30 \text{ m}$, grain size $D_G = 0.3 \text{ mm}$, $\mathbf{b} = 1.3$ (repose angle of 37.5°), $\mathbf{r}_s = 2650 \text{ kg/m}^3$, $\mathbf{r} = 1000 \text{ kg/m}^3$ and $\mathbf{e}_p = 0.375$. In the model, the vertical dimension z is described by 15 layers, distributed logarithmically, whereas the numerical errors are kept constant in all the computations (constant CFL number and 24 grid points per bottom perturbation wavelength). Furthermore, the width of the computational domain is equal to the wavelength of the studied bedform.

Regarding, the classification of van Rijn regarding the bed shear stress, these parameters implies a particle diameter parameter $D_* = 7.6$ and a Froude number $Fr < 0.8$. Thus, ripples, megaripples and dunes should be formed.

3. Instability and bed roughness: from dune to megaripple generation

From the numerical results, we estimate $\mathbf{w}(k)$, the complex growth rate of the bed perturbations of wavenumber k such that $\partial \tilde{h}_1 / \partial t = \mathbf{w} \tilde{h}_1$, where $\tilde{h}_1(k, t)$ is the first order Fourier transform of the bed perturbation $h_1(x, t)$. The amplification rate of the bottom perturbation is the real part of \mathbf{w} which is computed using the initial and final bathymetry obtained from the numerical model (Fig.2a). Here, we investigate the variation of the wavelength of the linearly most amplified mode, versus the bed roughness length. We focus first on the bedform generation for a flat bed where the bed roughness is equal to the grain roughness, then on the critical bed roughness for which megaripples of 20 m wavelength can be the linearly most amplified mode.

3.1 Results analysis

First, for a ripple-free bottom (grain related bed roughness length of 0.003 cm), among the studied wavelength range [10 m - 500 m], a single linearly most amplified mode ($I = 400\text{ m}$) is observed (Fig. 2a, first curve). Its wavelength lies in the range [100 m - 600 m] of observed dunes in the south of the North Sea (Stride, 1982). In addition, the small wavelength perturbations ($I < I_c$ with $I_c = 175\text{ m}$) are damped.

Then, additional computations are performed in order to analyze whether small-scale bedforms such as megaripples can grow if ripples are present on the sandy bed, as conjectured by (Richards, 1980). For that purpose, the bedform-related form roughness height k_{bf} is included in the bed roughness k_s . Increasing k_s , the linearly most amplified mode is shifted toward the short wavelengths. Interpolating the results (Fig. 2a), we obtain that the 20 wavelength megaripples are the most amplified mode for a bed roughness length of 3.6 cm, i.e. a bed roughness height k_{sc} of 1.1 m (Fig. 2a). These results also show that the megaripple growth rate (h^{-1}) is several orders of magnitude larger than the dune rates ($10^{-7} h^{-1}$): small bedforms are more dynamic than larger ones (Fig. 2b). Especially, regarding the dune observed in the middle of the Dover Strait (Fig. 1), the dune has a wavelength of 160 m for a long-term migration of 10 m/y, whereas the overlapping megaripples have a wavelength of 20 m for a migration of the order of 1 m/h. Then, from these observations, the time scale ratio is about 10^{-4} . Using the model results for these two wavelengths of 160 and 20 m (Fig. 2b), we obtain a ratio of $10^{-5} - 10^{-4}$. Thus, in term of magnitude order of the morphological time, our results are consistent with field observations.

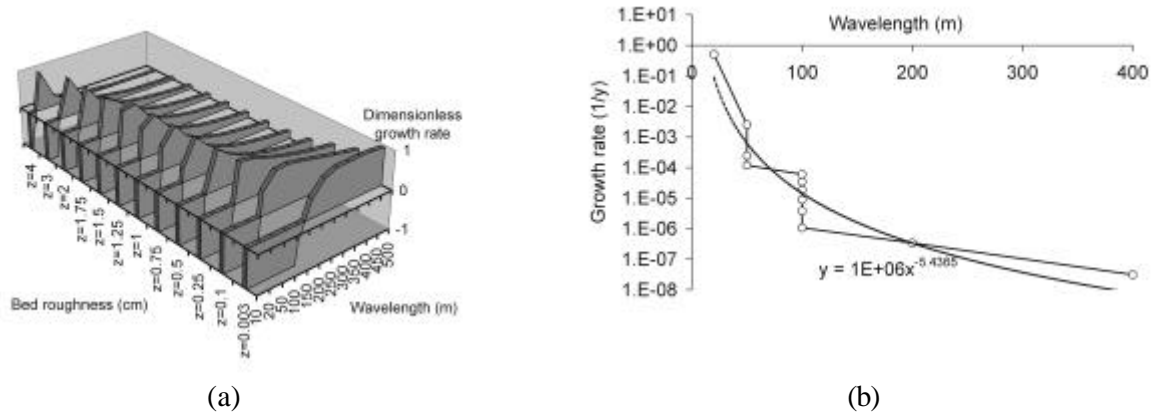


Fig. 2 – Growth rate versus bed roughness length z_0 . (a): dimensionless growth rate (for each bed roughness length z_0 , the growth rate is scaled with the maximum growth rate). (b): dimensional growth rate of the LMA mode (direct and interpolated results).

After some algebra (Idier and Astruc, 2003b), the growth rate can be related to the bed shear stress:

$$w_g = \frac{a(|t_{b0}| - t_c)^b}{1 - e_p} \left(\underbrace{\frac{b|t_{b1}|}{(|t_{b0}| - t_c)|h_1} \sin j_{t_b}}_A - \underbrace{bk|h_1}_B \right)$$

The values of t_{b0} , $|t_{b1}|$, and φ are plotted on Fig 3.

First, Fig. 3c shows that the phase-lag is always positive, larger than 180 degrees. Thus, the term A is always positive and is a growth term, whereas the bed slope effect ($-B$) is a damping term. From Fig 3a, the zeroth order bed shear stress t_{b0} increases with the bed roughness z_0 (i.e. k_s), but not with the

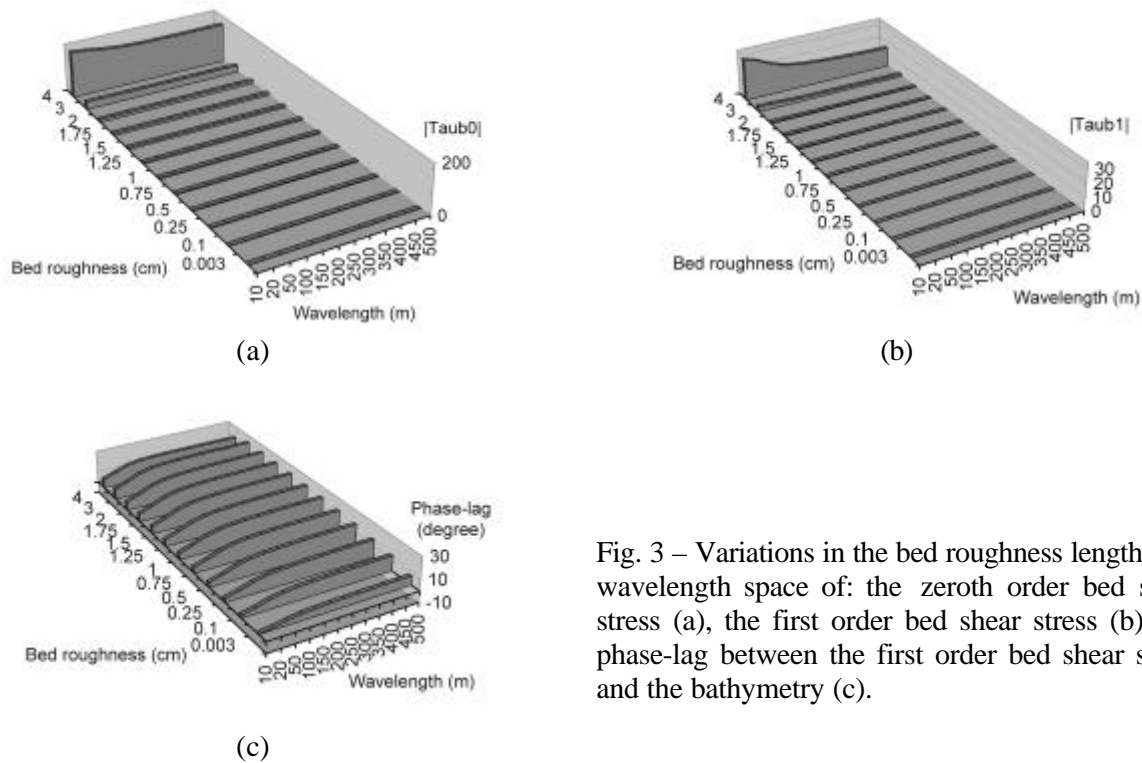


Fig. 3 – Variations in the bed roughness length z_0 – wavelength space of: the zeroth order bed shear stress (a), the first order bed shear stress (b), the phase-lag between the first order bed shear stress and the bathymetry (c).

wavelength. Thus, it will only contribute to the dynamics of the system, but not directly on the wavelength selection. Fig. 3b shows that the first order bed shear stress increases with the bed roughness, but decreases with the wavelength. Thus, this first order bed shear stress module contributes to the wavelength selection. From Fig. 3c, the phase-lag increases with increasing wavelength and bed roughness. Thus, for a fixed bed roughness, the phase-lag contributes to the selection of larger wavelength, compared to the wavelength obtained with smaller bed roughness.

3.2 Generation of megaripples: physical processes

In this section, we try to provide physical explanation for the obtained high bed roughness height of 1.1 m, and its corresponding bed shear stress t_{b0} , necessary for the generation of 20 m wavelength megaripples.

An increase in the bed roughness leads to a decrease in the wavelength of the most amplified mode: dunes are shifted toward megaripples. According to our numerical computations, the minimal bed roughness height is such that $k_{sc} = 1.1$ m, in 30 m water depth and $U=1$ m/s.

By interpolation of the results obtained for various bed roughness lengths we obtain a corresponding zeroth order bed shear stress of about 125 kg/m/s. Then, what are the mechanisms, related to such high bed roughness and such high bed shear stress, which could explain the megaripple generation? In order to answer to this question, we investigate the influence of the bedforms and the surface waves on bed roughness height (Tab. 2).

Generation of megaripples on a flat bed, by self interaction (coalescent mode)

The bed roughness height is about 1 m. Knowing that the studied 20 m megaripples reach an height of 1 to 2 m (Fig. 1), such bed roughness height corresponds to the roughness induced by the megaripple itself. Regarding the study of Richards (1980), it would mean that these megaripples correspond to the coalescent mode (convergence of dune and ripple modes toward one common mode).

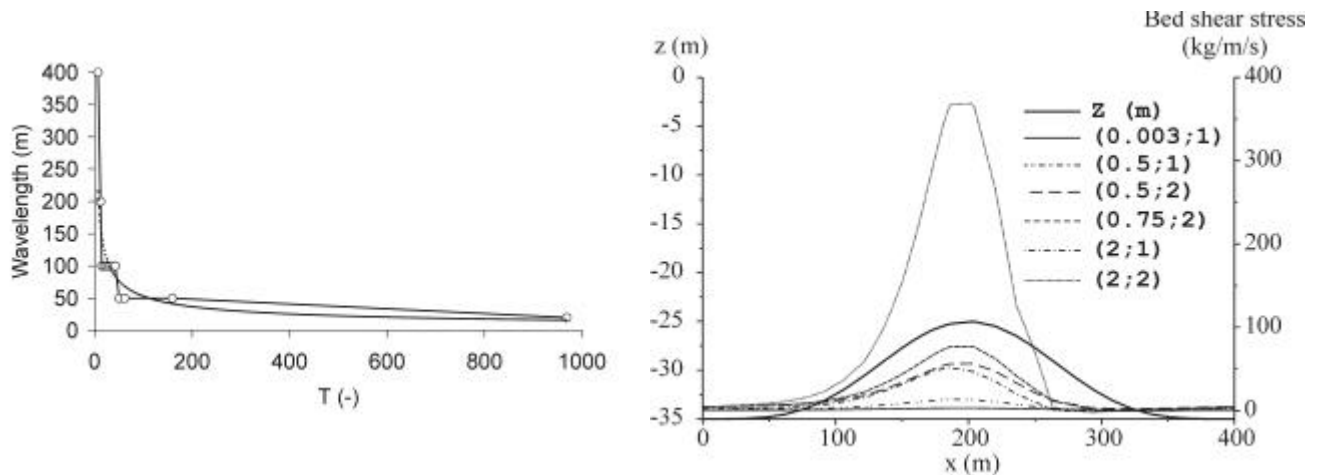


Fig. 4 – Bed shear stress. (a): parameter T of the LMA mode (direct and interpolated results), (b): Bed shear stress over finite amplitude dunes for different sets of (z_0 in cm ; U in m/s)

Case	Grain	Waves	Ripples	Megaripples	Waves + ripples	Waves + megaripples
ks (m)	0.0009	0.009	0.2	1	2	10
Water depth H_c (m)	15	17	24	30	33	45

Tab. 2 – Characteristic bed roughness height versus the marine environment, for fixed water depth of 30 m and depth integrated velocity of 1 m/s. The water depth H_c is the water depth required for a bed shear stress equal to the bed shear stress required for megaripples generation in 30 m water depth.

Generation of megaripples on a flat bed, by action of small bedforms and surface waves

As it has been seen in the previous computations, megaripples cannot be generated for a flat bed (no ripples), a water depth of 30 m and a velocity of 1 m/s. Then, we investigate the combinations water depth – ripples – surface waves for which the bed shear stress is equal to the bed shear stress required for megaripples generation in 30 m water depth. For this purpose, we use a bed roughness height of 20 cm to take into account the ripples, whereas the surface wave action is taken into account by multiplying the bed roughness by 10. Indeed, observations show that surface waves generate an apparent bed roughness, which is 1 to 10 (sometimes 100) times larger than the physical bed roughness (Perlin and Kit, 2002). Then, for a water depth of 30 m and a velocity of 1 m/s, only the combined action of ripples and surface waves could lead to megaripple generation. In smaller water depth, we assume that the water discharge is conserved ($Q=30$ kg/m/s) and estimate the water depth required to obtain the bed shear stress required for the megaripples generation in 30 m water depth. The results (Tab. 2) show that megaripples could be generated on flat bed, by the action of grain roughness only ($H=15$ m), surface wave roughness ($H=17$ m), or ripples roughness ($H=24$ m). For larger water depth (>30 m), we can notice that the combined action of ripples and surface waves would lead to megaripple generation.

Generation of megaripples on dunes

The 20 m wavelength megaripples are amplified for a zeroth order bed shear stress of 125 kg/m/s (Fig. 4a). This value implies that the bed shear stress parameter T is larger than 25. From in-situ and laboratory measurements, such high shear stress corresponds to fully developed sandwave. Thus, the conjecture is that, for small bed shear stress (grain related bed roughness), the dunes start to grow. Then, when they reach finite amplitude, they imply locally large bed shear stress, implying the formation of megaripples.

This conjecture is checked by numerical computations over a field of fixed finite amplitude dunes (Fig. 4b). These dunes are trochoidal, stand in 30 m water depth, have an height of 10 m and wavelength of 400 m. The figure 4b shows the bed shear stress profile for different combinations of bed roughness length and depth integrated velocity. We observe that, near the dune crest, the bed shear stress can be larger than the bed shear stress required for megaripple generation (125 kg/m/s). It is larger only for high velocity (here, 2 m/s) and large enough bed roughness length z_0 (here 2 cm), which corresponds to combine action of ripples, surface waves and high current velocity. However, the uncertainty about the exact value of the bed roughness makes definitive conclusion difficult. However, we can notice that, in any case, taking into account only the grain roughness and assuming no surface waves does not lead to large enough bed shear stress for megaripple generation over the dune. Only a large enough velocity, the presence of ripples and surface waves can lead to such high bed roughness over the dune.

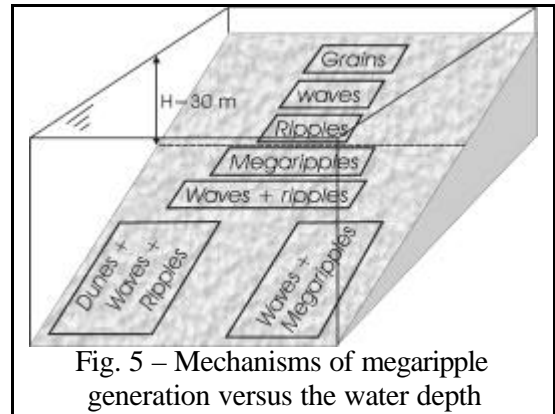


Fig. 5 – Mechanisms of megaripple generation versus the water depth

Further more, field observations show that, most of time, megaripples overlap entirely the dunes (especially the gentle slope) and are covered by ripples (Le Bot, 2001). In addition, Idier et al. (2002) observed that, during quite weather periods, the dune grows and the megaripples disappear. Initially, this observation has been interpreted as the result of avalanches along all the slope of the dune. Regarding the present numerical results on the megaripple generation, this interpretation can be completed. With the avalanche interpretation, a problem was to explain how these avalanches can cover all the length of the steep and gently slope of the dune. This could explain the damping of megaripples at the crest of the dune, but hardly at the foot of the gentle slope. Regarding the bed shear stress profile (Fig. 4b), we can deduce that, depending on current, ripples and waves, there is no direct generation of megaripples on a large part of the dune, except at the crest. However, the field observations show that megaripples are present over all the dune, but their height decrease from the dune crest toward the feet. Thus, we make the following conjecture: one of the mechanisms of dune-megaripples interaction could be that the presence of dune, in presence of ripples, larger enough current and surface waves, lead to megaripple generation at the dune crest. From this dune crest, megaripples are migrating and progressively damped toward the feet of the dune (Fig. 6a). This conjecture deals only with area where megaripples cover dunes, but not the flat bed in between the dunes. In other locations, where the water depth is smaller (Terwindt, 1971), the megaripples cover all the area. In this case, the megaripples do not strongly evolved between the dune foot and the dune crest. Thus, we assume that dunes are not directly responsible for megaripple formation (Fig 6b).

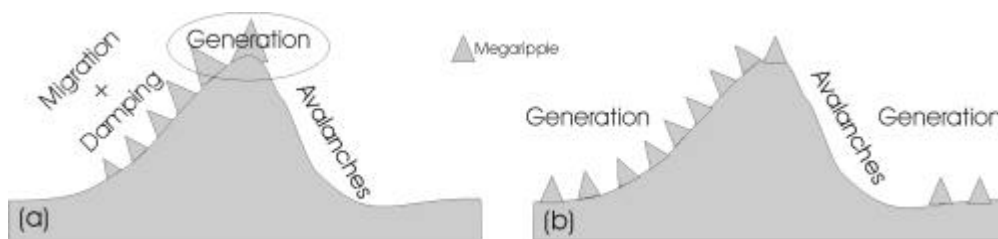


Fig. 6 – Megaripple dynamics on migrating dunes (from left to right).

4. Conclusion

This study of stability of the seabed shows that for increasing bed roughness the linearly most amplified mode is shifted from a dune mode of 400 m wavelength for grain roughness toward a megaripple mode of 20 m for a bed roughness height k_s of about 1 m. The interpretation of this high bed roughness value leads to propose various mechanisms of megaripple generation, depending not only on the water depth, but also

the presence of ripples, surface waves and dunes. From the coast toward the dune areas, the megaripples could be successively generated by: grain roughness, surface waves, ripple, other megaripples, combined ripples and surface waves. Then, in larger water depth, we propose the two following mechanisms: generation by dunes, surface waves and ripples, or generation by surface waves and other megaripples. We can notice that these results, which come from a linear stability analysis, but are supported by field observations, are in contradiction with the cascade concept, which states that dunes may result from megaripples (Flemming, 2000). However, our study needs further investigations in order to assess the megaripples mechanisms we propose. Especially, it would be worthwhile to: (1) perform stability analysis of a dune in equilibrium with the flow and determine whether megaripples are stable or unstable modes for this basic state, (2) perform extended bathymetric data analysis to correlate megaripples to ripples, water depth, surface waves and dunes.

Acknowledgment

The authors would like to thank Suzanne Hulscher for fruitful discussions and the French Hydrographic Service (SHOM), the CNRS and the European project EUMARSAND for financial support.

References

- R.W. Dalrymple, R.J. Knoght, J.J. Lambiase, Bedforms and their hydraulic stability relationship in a tidal environment, Bay of Fundy, Canada, *Nature*, Vol. 275, pp 100-104, 1978.
- N.W. Flemming, On the dimensional adjustment of subaqueous dunes in response to changing flow conditions: a conceptual process model. in *Proceedings of the Marine Sandwave Dynamics Workshop*, edited by A. Trentesaux and T. Garlan, 101-108, SHOM, Lille, France, march 2000.
- S.J.M.H. Hulscher, Tidal-induced large-scale regular bed form patterns in a three-dimensional shallow-water model, *J. of Geophys. Res.*, Vol. 101, C9, 20,727-20,744, 1996.
- D. Idier, Dynamique des bancs et dunes de sable du plateau continental: observations in-situ et modélisation numérique, PhD thesis, Institut National Polytechnique de Toulouse, 2002. (in french).
- D. Idier and D. Astruc, Analytical and numerical modeling of large-scale rhythmic bedform dynamics, *J. of Geophys. Res.*, Vol. 108, C3, 2003a.
- D. Idier and D. Astruc. Short-term dynamics of a Dover Strait tidal sandwave covered by megaripples. *3rd IAHR conference "River, Coastal and Estuarine Morphodynamics"*, Barcelone, Spain, pp 445-455, sept. 2003b.
- D. Idier, Ehrhold, A., and T. Garlan, Morphodynamics of an undersea sandwave of the Dover Strait, *C. R. Geoscience*, Vol. 334, 1079-1085, 2002.
- J.M. Janin, F. Marcos and T. Denot, Code Telemac-3D - Version 2.2 - Note théorique, Technical report E-42/97/049/B, EDF/LNH, 1997.
- S. Le Bot, Morphodynamique de dunes sous-marines sous influence des marées et des tempêtes. Processus hydro-sédimentaires et enregistrement. Exemple du Pas-de-Calais, PhD thesis, Université de Lille 1, 2001. (in french).
- S. Le Bot, J.P. Herman, A. Trentesaux, T. Garlan, S. Berné, and H. Chamley, Influence des tempêtes sur la mobilité des dunes tidales dans le détroit du Pas-de-Calais, *Oceanologica Acta*, Vol. 23(2), 129-141, 2000.
- A. Perlin and E. Kit, Apparent roughness in wave-current flow: implication for coastal studies, *Journal of Hydraulic Engineering*, August, pp 729-741, 2002.
- Richards, K., The formation of ripples and dunes on an erodible bed., *J. Fluid Mech.*, Vol. 99, 3, 597-618, 1980.
- A.H. Stride, Offshore tidal sands, Chapman and Hall, ISBN 0-412-129701, 1982.
- J. Terwindt, Sand waves in the southern bight of the North Sea. *Marine Geology*, Vol 10, pp 51-67, 1971.
- L.C. van Rijn, *Handbook of sediment transport by currents and waves*, 1002 pp., Report H 461, Delft Hydraulics, 1993.